

Monte Carlo Calculations on Intranuclear Cascades. II. High-Energy Studies and Pion Processes*†

N. METROPOLIS,‡ R. BIVINS, AND M. STORM,§ *Los Alamos Scientific Laboratory, Los Alamos, New Mexico*
J. M. MILLER, *Columbia University, New York, New York*
G. FRIEDLANDER, *Brookhaven National Laboratory, Upton, New York*

AND

ANTHONY TURKEVICH, *Enrico Fermi Institute for Nuclear Studies, University of Chicago, Chicago, Illinois*

(Received December 9, 1957)

The nuclear cascade calculations described in the preceding paper have been extended to incident energies up to 1.8 Bev with the inclusion of pion production, scattering, and absorption processes. Again the MANIAC electronic computer was used. Several incident proton energies between 450 Mev and 1.8 Bev have been investigated, with Al^{27} , Cu^{64} , Ru^{100} , Ce^{140} , Bi^{209} , and U^{238} as target nuclei. Cascades initiated by pions of several energies up to 1500 Mev incident on Ru^{100} have also been studied. The elementary cross sections used and the assumptions made about details of the inelastic nucleon-nucleon and pion-nucleon processes are presented. The results of the calculation are summarized in tables and graphs giving data on transparencies, on numbers, energy spectra, and angular distributions of emitted cascade nucleons and pions, and on frequencies of occurrence and excitation energies of residual nuclei. The computed number distributions, energy spectra, and angular distributions of emitted particles are compared with the results of several emulsion experiments with incident protons and negative pions. The agreement is generally satisfactory, but certain discrepancies are found, for example regarding spectra and angular distributions of emitted pions; some of these discrepancies are discussed in terms of details of the model used. The calculation predicts quite well the over-all yield distribution of spallation products of copper produced by 2-Bev protons; however, as at lower energies, the calculated cross sections for (p, pn) reactions are too low by factors of two or three.

NUCLEAR MODEL AND INPUT INFORMATION

THE nuclear cascade calculations described in the preceding paper¹ have been extended to the interval 0.4–1.8 Bev in incident nucleon energy. Pion production (single or double), pion scattering and charge exchange, and pion absorption have been included with varying degrees of completeness and accuracy. The angular distributions in nucleon-nucleon scattering, pion-nucleon scattering and charge exchange have also been taken into account. Cascades induced by incident pions have also been investigated. This appears to be the first extensive attempt to carry such calculations into the energy region in which pion effects are important. However, after the completion of the present computation, Nikol'skii *et al.*² have published some results of a Monte Carlo cascade calculation involving 162-Mev π^- mesons incident on emulsion nuclei.

As in I, the calculations were performed relativistically in three-dimensional geometry by means of the MANIAC electronic computer at Los Alamos. The

nuclear characteristics chosen for the target nuclei were the same as in I, with the radius parameter r_0 always taken as 1.3×10^{-13} cm. Neutrons, protons, and the three types of pions were distinguished throughout. The mass of all the pions was taken as one-seventh of the nucleon mass. No nuclear or electrostatic potential was included for the pions, and Coulomb scattering was neglected for all particles.

The behavior of each cascade nucleon was followed as long as its kinetic energy was above an assumed "cutoff energy" as described in I. Cascade pions were followed until they either were absorbed or escaped from the nucleus.

The total elementary cross sections for nucleons above 335 Mev and for pions above 51 Mev were put into the computer in the form of a table with entries at 8 unequally spaced energies. Table I shows these

TABLE I. Total cross sections used in cascade calculation. The quantities σ_{ii} , σ_{ij} , and $\sigma_{ij(aba)}$ are defined in the text.

Kinetic energy (Mev)	Nucleons		Pions			
	σ_{ii}^a (mb)	σ_{ij}^b (mb)	Kinetic energy (Mev)	σ_{ii}^c (mb)	σ_{ij}^c (mb)	$\sigma_{ij(aba)}^d$ (mb)
335	24.5	33.0	49	16	15	20
410	26.4	34.0	85	50	21	32
510	30.4	35.1	128	114	43	45
660	41.2	36.5	184	200	66	36
840	47.2	37.9	250	110	44	18
1160	48.0	40.2	350	51	23	0
1780	44.2	42.7	540	20	22	0
3900	41.0	42.0	1300	30	30	0

^a Based on data from references 3 to 9.

^b Based on data from references 3, 9 to 12.

^c Based on data from references 13 and 14.

^d Based on data from references 15 to 19.

* This work was supported in part by the U. S. Atomic Energy Commission.

† A preliminary report of this work was presented at the January, 1957, New York Meeting of the American Physical Society [G. Friedlander *et al.*, Bull. Am. Phys. Soc. Ser. II, 2, 63 (1957)].

‡ Now with Institute for Computer Research, University of Chicago, Chicago, Illinois.

§ Now with Midwestern Universities Research Association (MURA), Madison, Wisconsin.

¹ Metropolis, Bivins, Storm, Turkevich, Miller, and Friedlander, Phys. Rev. **110**, 185 (1958), preceding paper, henceforth referred to as I.

² Nikol'skii, Kudrin, and Ali-Zade, J. Exptl. Theoret. Phys. U.S.S.R. **32**, 48 (1957) [translation: Soviet Phys. JETP **5**, 93 (1957)].

elementary cross sections which, together with the nuclear constitution and size, were used to calculate the mean free paths of nucleons and pions in nuclear matter. Columns one and four give the kinetic energies of the nucleons and pions, respectively (in a system in which the struck nucleons are at rest). Column two, labeled σ_{ii} , gives the values of the total p - p and n - n cross sections used, as obtained from various experimental data.³⁻⁹ Column three, labeled σ_{ij} , gives the values of the total n - p cross sections derived in part from direct measurements,^{10,11} but mostly based on the differences between p - d and p - p cross sections^{3,9} treated in a manner suggested by Glauber.¹² Below 335 Mev, meson production by nucleons was neglected and the nucleonic cascade was followed as described in I. In Fig. 1 the total nucleon-nucleon cross sections used are compared with experimental data; linear interpolation was used between the points given in Table I.

For the pions, σ_{ii} is the cross section for π^- - n and π^+ - p collisions, σ_{ij} that for π^- - p and π^+ - n collisions (not including absorption processes). Columns five and six of Table I list these pion-nucleon cross sections.^{13,14} Meson absorption was assumed to occur via a two-nucleon mechanism, and column seven gives the effective cross section for absorption, $\sigma_{ij(\text{abs})}$.¹⁵⁻¹⁹ This quantity was defined as the cross section for the absorption of a charged pion by a nucleon with isotopic spin projection of the opposite sign (i.e., a pair of nucleons must contain at least one proton to absorb a π^- , at least one neutron to absorb a π^+). The absorption cross section, $\sigma_{ij(\text{abs})}$, was estimated from the cross section for the absorption of pions by deuterons in a manner suggested by Brueckner, Serber, and Watson.¹⁵ Isotopic spin considerations indicate that the absorption

cross section for π^0 mesons should be $\frac{1}{2}\sigma_{ij(\text{abs})}$. To determine mean free paths for pions, the sum of absorption and scattering cross sections was used.

Analytic expressions were devised to represent both the scattering and the absorption cross sections for pions with energies below 51 Mev. The total pion-nucleon scattering cross sections (σ_{ii} and σ_{ij}) were taken from the estimates of Anderson, Davidson, and Kruse²⁰ for this energy region and increases made for the effect of nucleon motion in the manner indicated in I for the nucleon-nucleon cross sections. The absorption cross section data were taken from Frank, Gammel, and Watson.²¹ If the cross sections are expressed in mb, the total energies (γ) in units of $m_\pi^0 c^2$, and the momenta (η) in units of $m_\pi^0 c$, the analytic equations giving the cross sections are:

$$\sigma_{ii} = 3.7 + 286(\gamma - 1)^3, \quad (1)$$

$$\sigma_{ij} = 6.5 + 23.9(\gamma - 1), \quad (2)$$

$$\sigma_{ij(\text{abs})} = 16.4(0.14 + \eta^2)/\eta. \quad (3)$$

In Fig. 2 the total pion-nucleon cross sections used in the calculation are compared with experimental data. Again, linear interpolation between the energies of Table I was used, and for all pions of energy greater than 1.3 Bev, the cross section for both ii and ij collisions was taken to be 30 mb. Because of the limitations imposed by the computer memory, the higher-energy resonances in pion-nucleon interactions¹⁴ were ignored.

³ Chen, Leavitt, and Shapiro, Phys. Rev. **103**, 212 (1956), and C. Leavitt (private communication).

⁴ Smith, McReynolds, and Snow, Phys. Rev. **97**, 1186 (1955).

⁵ Morris, Fowler, and Garrison, Phys. Rev. **103**, 1472 (1956).

⁶ Fowler, Shutt, Thorndike, and Whittemore, Phys. Rev. **103**, 1479 (1956).

⁷ Block, Harth, Cocconi, Hart, Fowler, Shutt, Thorndike, and Whittemore, Phys. Rev. **103**, 1484 (1956).

⁸ Dzhelepov, Moskalev, and Medved, Doklady Akad. Nauk S.S.S.R. **104**, 380 (1955).

⁹ Shapiro, Leavitt, and Chen, Phys. Rev. **95**, 663 (1954).

¹⁰ V. Nedzel, Phys. Rev. **94**, 174 (1954).

¹¹ Coor, Hill, Hornyak, Smith, and Snow, Phys. Rev. **98**, 1369 (1955).

¹² R. J. Glauber, Phys. Rev. **100**, 242 (1955). The numerical values of the corrected p - n cross section used here differ somewhat from those given in reference 3 although both sets are based on the same experimental data and on Glauber's correction term; however, a different constant in the correction term was used here to give agreement with the measured n - p cross sections at 410 Mev and 1400 Mev.

¹³ L. C. L. Yuan and S. J. Lindenbaum, Phys. Rev. **100**, 306 (1955).

¹⁴ Cool, Piccioni, and Clark, Phys. Rev. **103**, 1082 (1956).

¹⁵ Brueckner, Serber, and Watson, Phys. Rev. **84**, 262 (1951).

¹⁶ Meshcheriakov, Bogachev, and Neganov, Izvest. Akad. Nauk S.S.S.R. Ser. Fiz. **19**, 548 (1955).

¹⁷ F. S. Crawford and M. L. Stevenson, Phys. Rev. **97**, 1305 (1954).

¹⁸ H. L. Stadler, Phys. Rev. **96**, 734 (1954).

¹⁹ R. A. Schluter, Phys. Rev. **96**, 734 (1954).

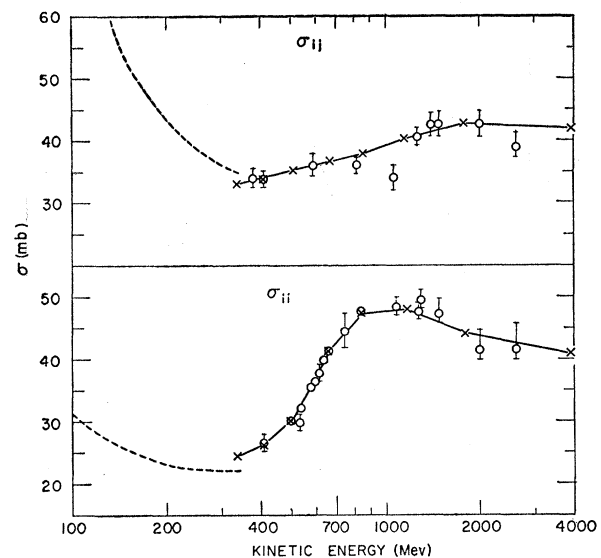


FIG. 1. Total nucleon-nucleon cross sections as a function of nucleon kinetic energy. The top graph (labeled σ_{ij}) shows the n - p cross section, the bottom graph (labeled σ_{ii}) shows the n - n and p - p cross section. Experimental points are shown by the open circles, the values used in the calculation by the crosses and by the lines connecting them. The analytic functions used at energies below 335 Mev (see I) are indicated by the dotted curves.

²⁰ Anderson, Davidson, and Kruse, Phys. Rev. **100**, 339 (1955).

²¹ Frank, Gammel, and Watson, Phys. Rev. **101**, 891 (1956).

This should have little effect on the results because the production of very-high-energy pions is quite infrequent.

The cross sections for π^0 -nucleon interactions were taken to be the same for protons and neutrons and equal to the arithmetic mean of the π^+ and π^- cross sections at the same energy. For pion energies above 51 Mev these cross sections were supplied in tabular form along with the π^+ and π^- cross sections.

The parameters involved in the kinematics of the collisions were treated more crudely and were taken as constant within each of eight energy regions. For nucleon-nucleon collisions the parameters used are summarized in Table II. The energy of the collision in the center-of-mass system was calculated from the kinetic energies of the incident and struck particles and their relative directions of motion. The incident kinetic energy which would give rise to the same center-of-mass energy was then computed for a nucleon striking a stationary nucleon, and the collision parameters corresponding to this kinetic energy were taken from Table II. The energy ranges are listed in column one. Column two gives the type of the collision (*ii* or *ij*). Column three shows the fraction (f_{inel}) of the total cross section that was taken as involving pion production.^{4-7,22,23} Columns four and five give the coefficients

of the angular distribution of the elastic scattering in the center-of-mass system when it is expressed in the form

$$d\sigma/d\Omega \approx A \cos^4\theta + B \cos^2\theta + 1. \quad (4)$$

The particular values of A and B chosen were obtained by a least-squares fit to the experimental data.^{4,24-28} The last column indicates the fraction (f_π) of the meson production that is single pion production.^{5-7,23} The remainder ($1-f_\pi$) was assumed to be double pion production. Because of the paucity of available data, f_π was taken to be independent of the collision type.

In single pion production, 11%^{5-7,23,29,30} was taken as the fraction producing neutral pions in *ii*-type collisions at all energies. In *ij*-type collisions the corresponding fraction was taken as 43%.³¹ In double pion production, 80% of the cases were taken as producing either two neutral pions or a $\pi^+\pi^-$ combination,²³ with the former occurring three times as often as the latter.

TABLE II. Parameters used in inelastic nucleon-nucleon collisions.

Energy range (Mev)	Type	f_{inel}^a	A^b	B^b	f_π^c
335-410	<i>ii</i>	0.07	0.1	0	1.0
	<i>ij</i>	0.04	2.2	-1.0	1.0
410-510	<i>ii</i>	0.20	0.9	0	1.0
	<i>ij</i>	0.07	1.8	-1.1	1.0
510-660	<i>ii</i>	0.31	2.7	0	1.0
	<i>ij</i>	0.15	2.3	-0.7	1.0
660-840	<i>ii</i>	0.43	9.0	0	1.0
	<i>ij</i>	0.27	8.8	-0.2	1.0
840-1160	<i>ii</i>	0.58	14.3	0	0.97
	<i>ij</i>	0.37	15.0	0	0.97
1160-1780	<i>ii</i>	0.65	19.2	0	0.80
	<i>ij</i>	0.36	29.4	0	0.80
>1780	<i>ii</i>	0.69	∞	0	0.44
	<i>ij</i>	0.35	∞	0	0.44

^a Based on data in references 4-7, 22, 23.

^b Based on data in references 4, 24 to 28.

^c Based on data in references 5-7, 23.

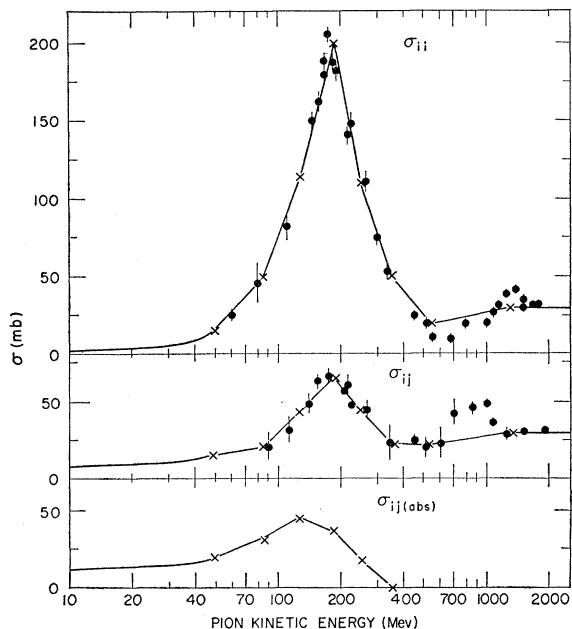


FIG. 2. Pion-nucleon cross sections as a function of pion kinetic energy. The cross section for π^-n or π^+p collisions is denoted by σ_{ii} , that for π^+n or π^-p collisions by σ_{ij} . $\sigma_{ij(abs)}$ is the absorption cross section for charged pions (see text). Experimental points are shown by solid circles, the values used in the calculation by the crosses and by the lines connecting them.

²² E. Fowler (private communication).

²³ Fowler, Shutt, Thorndike, and Whittemore, Phys. Rev. **95**, 1026 (1954).

The assumptions made here about the distributions of produced pions among the three charge types are doubtless not very reliable. They were based on the fragmentary data in the references and on isotopic spin considerations. The effects of this unreliability in the input data should not be serious, however, because the interaction cross sections of neutral pions were taken as the average of those for charged pions and also because charge exchange scattering occurs frequently.

The parameters used to describe the details of the pion-nucleon collisions are listed in Table III. As in

²⁴ Marshall, Marshall, and Nedzel, Phys. Rev. **92**, 834 (1953).

²⁵ Mott, Sutton, Fox, and Kane, Phys. Rev. **90**, 712 (1953).

²⁶ B. Cork and W. A. Wentzel, Phys. Rev. **100**, 962 (1955).

²⁷ Kelly, Leith, Segrè, and Wiegand, Phys. Rev. **79**, 96 (1950).

²⁸ Hartzler, Siegel, and Opitz, Phys. Rev. **95**, 591 (1954).

²⁹ Fields, Reiter, and Sutton, Bull. Am. Phys. Soc. Ser. II, **1**, 71 (1956).

³⁰ Stallwood, Fields, Fox, and Kane, Bull. Am. Phys. Soc. Ser. II, **1**, 71 (1956).

³¹ E. Fermi, Phys. Rev. **92**, 452 (1953); **93**, 1434 (1954).

Table II, the energy range listed in column one is that of a pion hitting a stationary nucleon. Column two indicates the type of the interaction, ii or ij , as before. The symbol 0 refers to interactions involving π^0 mesons. Column three indicates the fraction (f_{inel})³²⁻³⁴ of the total cross section that involves inelastic processes including charge exchange. Column four gives the fraction (f_{CE}) of the inelastic events that is charge exchange. The next two columns (five and six) indicate the coefficients A and B of the angular distribution for elastic pion-nucleon scattering in the center-of-mass system according to Eq. (4).³⁵⁻³⁹ In charge exchange scattering, the angular distribution was taken to be the same as in ii scattering.

TABLE III. Parameters used in pion-nucleon collisions.

Energy range (Mev)	Type	f_{inel}^a	f_{CE}^b	A^c	B^c	f_{π^a}
49-85	ii	0	0	3.2	-1.8	1.00
	ij	0.45	1.0	1.1	0.8	
	0	0.42	1.0	3.4	-1.8	
85-128	ii	0	0	2.2	-2.1	1.00
	ij	0.57	1.0	1.9	0.7	
	0	0.36	1.0	2.1	-2.0	
128-184	ii	0	0	1.9	-1.5	1.00
	ij	0.62	1.0	2.2	0.8	
	0	0.36	1.0	1.9	-1.4	
184-250	ii	0.03	0	2.2	-0.3	1.00
	ij	0.64	0.95	2.2	1.0	
	0	0.37	0.90	2.1	0	
250-350	ii	0.06	0	2.6	2.0	1.00
	ij	0.62	0.89	2.0	1.4	
	0	0.40	0.84	2.5	1.7	
350-540	ii	0.16	0	3.0	4.0	0.98
	ij	0.56	0.72	2.7	2.6	
	0	0.50	0.67	3.0	4.0	
540-1300	ii	0.30	0	3.0	4.0	0.91
	ij	0.58	0.51	3.0	3.6	
	0	0.59	0.50	3.0	4.0	
>1300	ii	0.88	0	3.0	4.0	0.24
	ij	0.94	0.06	3.0	4.0	
	0	0.94	0.05	3.0	4.0	

^a Based on data in references 32 to 34.

^b Estimated from isotopic spin formalism and data in reference 13.

^c Values of the angular distribution parameters A and B [Eq. (4)] are based on data in references 35 to 39.

The last column of Table III gives the fraction of pion production that was taken to be single pion production.³²⁻³⁴ In single pion production, 55%^{34,40} was taken to be π^0 production in ii -type collisions irre-

³² W. D. Walker and W. D. Shepherd, Phys. Rev. **100**, 1264(A) (1955).

³³ Eisberg, Fowler, Lea, Shepard, Shutt, Thorndike, and Whittemore, Phys. Rev. **97**, 797 (1955).

³⁴ V. P. Kenny, Bull. Am. Phys. Soc. Ser. II, **1**, 71 (1956).

³⁵ H. A. Bethe and F. de Hoffmann, *Mesons and Fields* (Row, Peterson and Company, Evanston, 1955), Vol. 2.

³⁶ Fowler, Lea, Shepard, Shutt, Thorndike, and Whittemore, Phys. Rev. **92**, 832 (1953).

³⁷ Ashkin, Blaser, and Feiner, Bull. Am. Phys. Soc. Ser. II, **1**, 72 (1956).

³⁸ Stern, Ashkin, Blaser, and Feiner, Bull. Am. Phys. Soc. Ser. II, **1**, 72 (1956).

³⁹ R. S. Margulies, Phys. Rev. **100**, 673(A) (1955).

⁴⁰ The value derived from reference 34 is 65%; 55% was used erroneously in the calculation.

TABLE IV. Coefficients for the angular distribution of pion-nucleon interactions below 51 Mev.

Collision type	A	B
ii	2.5	-3.5
ij	2.5	+3.5
0	3.0	-2.0
CE	1.5	-2.5

spective of the energy, and 44% of the events were assumed to lead to π^0 production in ij and in π^0 -nucleon collisions. This last number is the arithmetic mean between the values reported for 1.0-Bev³² and 1.4-Bev³³ π^- interactions with protons. In double pion production a quarter of the events were taken to make two neutral pions or a $\pi^+\pi^-$ pair, with the former occurring three times as often as the latter. The data on which these assumptions on pion production are based are even more fragmentary than those for nucleon-nucleon collisions; but again the results of the calculation are not expected to be sensitive to such details.

For pion energies below 51 Mev, charge exchange was assumed to occur in 80% of all those pion-nucleon interactions in which it was possible. The angular distribution coefficients of Eq. (4) for this energy range are given in Table IV, where the coefficients listed under CE refer to the angular distribution in charge-exchange collisions. These quantities describing pion-nucleon interactions below 51 Mev are averages over the energy range derived from the poorly known phase shifts.^{35,41,42}

A simplified arbitrary model was used for the dynamics of both single and double meson production: all resultant particles were assumed to have equal momenta in the center-of-mass system. The pion produced in single meson production was assigned a random direction in the plane of the reaction and then this plane was rotated randomly about the axis containing the reactants in the center-of-mass system. In double pion production, one pion direction was chosen randomly in the plane of the reaction, the other pion was taken to travel in the opposite direction, and the nucleon directions were chosen at right angles to the pion direction in the reaction plane. This plane was then randomly rotated about the axis containing the reactants in the center-of-mass system.

In the case of pion absorption, the two nucleons participating in the absorption were chosen randomly from the Fermi distribution, and the meson energy was distributed equally between the two in the center-of-mass system. The direction of motion of the resultant nucleons in this system was taken as isotropically distributed in space.

⁴¹ Orear, Slater, Lord, Eilenberg, and Weaver, Phys. Rev. **96**, 174 (1954).

⁴² Nagle, Hildebrand, and Plano, Phys. Rev. **105**, 718 (1957).

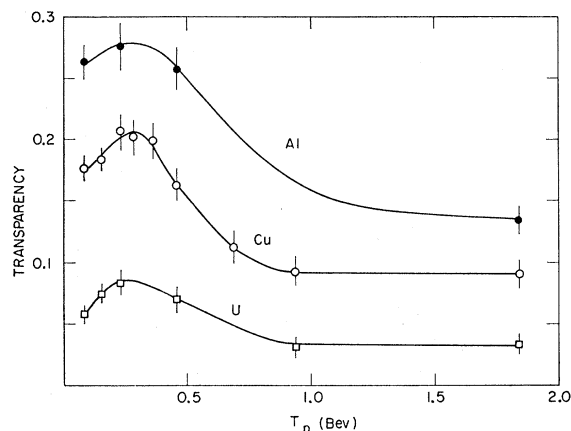


FIG. 3. Calculated transparencies of Al^{27} , Cu^{64} , and U^{238} for protons of various energies.

RESULTS

The particular combinations of targets and incident particles that have been investigated are listed in Table V. Usually 800 to 1000 cascades were followed for each case. The target nuclei investigated were, as in I, Al^{27} , Cu^{64} , Ru^{100} , Ce^{140} , Bi^{209} , and U^{238} . The incident energies were chosen to cover the range up to about 2 BeV and to allow comparison with experimental data from existing accelerators.

The output data for each cascade include the identity, energy, and angle of emission for each particle ejected from the nucleus during the cascade. In addition, there are recorded for each cascade the identity and excitation energy of the residual nucleus, and the number and momenta of the particles struck during the cascade process. Unfortunately it is not possible to present in this paper all the information obtained.

As in I, the computer has also been employed to scan the output data for each case and to compile from them information such as the number distributions, energy spectra, and angular distributions of the various kinds of outgoing particles, as well as the mass and charge distribution and excitation energy spectra of residual nuclei. Some representative results are reported in the following paragraphs.

Transparency.—The calculated nuclear transparencies of the various target nuclei for protons of several energies are shown in Table VI, and for Al, Cu, and U the transparencies are plotted as a function of energy (including the data of I) in Fig. 3. As is expected, the

TABLE V. Cases of "high-energy" cascades treated in the present investigation. (p , n , and π indicate incident protons, neutrons, and pions.)

Incident energy (Mev)	Target element					
	Al	Cu	Ru	Ce	Bi	U
0	π^-		π^-			π^-
50			π^-			
134			π^-			
179			π^-			
210			π^+			
460	p	p, n	p, π^-	p	p	p
690		p	p			
940		p	p		p	p
1500			π^-			
1840	p	p	p	p	p	p

transparency decreases with increasing mass number at a given incident energy. The energy dependence for a given target reflects the behavior of the input data for the nucleon-nucleon total cross sections. The pion transparencies of Ru^{100} are listed in Table VII. The transparency of Cu^{64} for 460 Mev neutrons turned out to be 0.170 ± 0.015 , equal within the error to the proton transparency at the same energy.

Average number of cascade nucleons emitted per interaction.—The dependence of the average number of emitted cascade nucleons upon the mass number of the target and the energy of the incident particle is given in Fig. 4. The relative insensitivity of this quantity to the mass number of the target is rather surprising; it is probably the result of the balancing of two related quantities: the increase with mass number of the number of nucleons involved in the cascade, and the decrease with mass number of the probability that any given cascade nucleon will escape from the nucleus. The monotonic increase of the average number of emitted nucleons with increasing bombarding energy is not unexpected.

Ratio of average number of emitted cascade protons to average number of emitted cascade neutrons.—The relative numbers of protons and neutrons ejected by the cascade process are indicated in Table VIII where the ratio of the average number of emitted neutrons to that of emitted protons is given. Data for the low-energy region are included (from I). The preponderance of neutron emission from heavy elements noted at lower bombarding energies persists at the higher energies also, probably for the reasons discussed in I. It is interesting to note that for uranium, where the cascade has the best chance of becoming fairly extensive, the average

TABLE VI. Calculated transparencies for protons.

Kinetic energy (Mev)	Al^{27}	Cu^{64}	Ru^{100}	Ce^{140}	Bi^{209}	U^{238}
460	0.257 ± 0.017	0.162 ± 0.013	0.140 ± 0.013	0.103 ± 0.011	0.083 ± 0.009	0.070 ± 0.009
690		0.112 ± 0.013				
940		0.093 ± 0.012	0.055 ± 0.009		0.053 ± 0.009	0.032 ± 0.007
1840	0.134 ± 0.012	0.090 ± 0.011	0.078 ± 0.014	0.053 ± 0.010	0.031 ± 0.007	0.037 ± 0.007

TABLE VII. Calculated transparencies for pions incident on Ru¹⁰⁰.

Particle	Kinetic energy (Mev)	Transparency
π^-	50	0.315 ± 0.017
π^-	134	0.008 ± 0.003
π^-	179	0.010 ± 0.004
π^+	210	0.013 ± 0.004
π^-	465	0.238 ± 0.017
π^-	1500	0.142 ± 0.018

ratio of neutron emission to proton emission is, over the whole energy range, greater than the neutron to proton ratio in the target nucleus. For each element the average ratio of cascade neutron to cascade proton emission goes through a flat minimum in the region of 200 to 400 Mev.

Pion emission.—The average number of pions emitted per inelastic event is shown in Fig. 5 for three incident proton energies and various target nuclei. Pion production is rather insensitive to the mass number of the target nucleus, probably because the increase in pion production with increasing nuclear size is compensated by the decrease in the probability for escape of the pions. Although the pion yields shown here depend upon pion production cross sections which are not too well known, and especially upon the assumptions made concerning the distribution of energy in pion production processes, it is not expected that the dependence on nuclear size shown in Fig. 5 would be significantly changed by more refined input data.

The calculated distribution of the pions produced in proton-induced cascades among the three charge types is shown in Table IX. These results show that, especially for high incident energies, charge exchange scattering goes a long way toward washing out any details assumed for the production processes. The average numbers of emitted pions (and neutrons) for pion-induced cascades are given in Table X.

Angular distributions of emitted nucleons and pions.—In Figs. 6 through 11 the angular distributions of emitted protons and pions for aluminum and uranium targets and for bombarding energies of 460 and 1840

TABLE VIII. Ratio of average number of cascade neutrons to average number of cascade protons emitted in proton-induced reactions.

Incident energy (Mev)	Al	Cu	Ru	Ce	Bi	U
82	0.84	1.04	1.20	1.82	1.67	2.08
158	...	0.96	1.15	1.96
239	0.74	0.93	1.10	1.43	...	1.61
290	...	1.00	1.12	...	1.64	...
365	...	1.00	...	1.33
460	0.79	1.02	1.16	1.43	1.59	1.89
690	...	1.02
940	...	1.16	1.22	...	1.89	2.00
1840	0.92	1.18	1.25	1.56	1.75	2.08

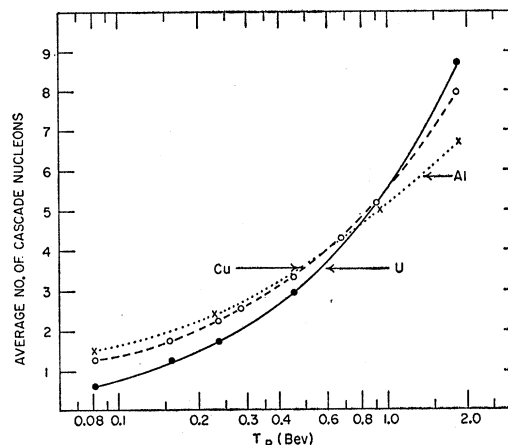


Fig. 4. Average number of emitted cascade nucleons per inelastic event plotted as a function of incident proton energy for three target elements.

Mev are shown. The input parameters describing the angular distribution in nucleon-nucleon scattering are considerably better known than those describing pion production and pion scattering; hence the nucleon angular distributions are doubtless more reliable than those for the pions. The angular distributions of emitted protons and neutrons are essentially indistinguishable.

The forward peaking of the cascade nucleon emission is clearly to be expected from the model. The strong forward and slight backward peaking of the emitted pions in the 1840-Mev interactions (Figs. 10 and 11) probably results from the fact that those pions produced in the forward and backward directions in the center-of-mass system, i.e., those with the highest and lowest energies, have much larger mean free paths than those with energies near the 180-Mev resonance peak. The absence of a forward peak in the pion distributions for

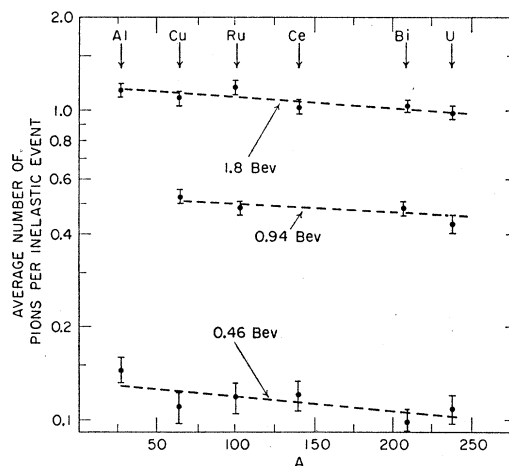


Fig. 5. Average number of pions (of all charge states) emitted per inelastic proton interaction with various target nuclei.

TABLE IX. Average number of pions of all types (π), and separately of π^0 , π^+ , and π^- mesons emitted per inelastic event in proton-induced reactions.

Target element	Pion type	Incident energy (Bev)			
		0.46	0.69	0.94	1.84
Al ²⁷	π	0.145±0.015			1.170±0.048
	π^0	0.049±0.009			0.516±0.032
	π^+	0.076±0.011			0.401±0.028
	π^-	0.019±0.005			0.253±0.022
Cu ⁶⁴	π	0.110±0.012	0.308±0.023	0.540±0.029	1.056±0.038
	π^0	0.035±0.007	0.113±0.014	0.196±0.018	0.483±0.026
	π^+	0.054±0.008	0.148±0.016	0.232±0.019	0.310±0.021
	π^-	0.021±0.005	0.047±0.009	0.112±0.013	0.263±0.019
Ru ¹⁰⁰	π	0.118±0.013		0.490±0.027	1.186±0.056
	π^0	0.036±0.007		0.184±0.017	0.501±0.036
	π^+	0.063±0.010		0.202±0.018	0.329±0.030
	π^-	0.019±0.005		0.103±0.013	0.355±0.031
Ce ¹⁴⁰	π	0.120±0.013			1.022±0.047
	π^0	0.031±0.007			0.461±0.032
	π^+	0.067±0.010			0.289±0.025
	π^-	0.022±0.006			0.272±0.024
Bi ²⁰⁹	π	0.099±0.010		0.524±0.028	1.030±0.043
	π^0	0.034±0.006		0.187±0.017	0.447±0.028
	π^+	0.042±0.007		0.176±0.016	0.270±0.022
	π^-	0.023±0.005		0.161±0.016	0.315±0.024
U ²³⁸	π	0.108±0.012		0.430±0.028	1.017±0.037
	π^0	0.044±0.008		0.164±0.017	0.427±0.024
	π^+	0.040±0.007		0.151±0.016	0.276±0.019
	π^-	0.025±0.006		0.114±0.014	0.314±0.020

the 460-Mev interactions (Figs. 10 and 11) is consistent with this explanation since, at this incident energy, pions with energies above the resonance region are not produced.

Energy spectra of emitted protons.—The energy spectra of the protons emitted during the cascade process are shown for aluminum and uranium targets and two extreme incident proton energies in Figs. 12 and 13. At both bombarding energies the proton spectra are shifted to lower energies for uranium as compared to aluminum, presumably because the greater cascade development in the larger nucleus leads to more energy degradation of the cascade nucleons. The spectra are remarkably insensitive to bombarding energy, with very few protons of energies in excess of 500 Mev emitted in the high-energy bombardments. The slight shoulder indicated at the high-energy end of the proton spectra from aluminum in Figs. 12 and 13 appears to be real. It is found in other calculated proton spectra,

but appears to decrease in importance with increasing bombarding energy and with increasing A .

Energy spectra of emitted pions.—Because of the relatively small numbers of emitted pions, only crude data on energy spectra can be given. The fractions of pions emitted in each of four energy intervals—0 to 45, 45 to 90, 90 to 200, and greater than 200 Mev—are given in Table XI for protons of several different energies incident on copper and uranium. Again, these results may be sensitive to the input parameters and assumptions; in particular, for high incident energies the assumed equipartition of momentum among the products of inelastic collisions probably gives rise to the emission of too many high energy pions.

Average excitation energy of residual nuclei.—The average excitation energy remaining in the struck nucleus (events without energy transfer are not included in the averaging) is shown in Fig. 14 as a function of proton bombarding energy for each of four different

TABLE X. Average numbers of cascade pions and nucleons emitted from Ru¹⁰⁰ interacting with incident pions of several energies.

Emitted particle	Incident particle				
	50-Mev π^-	134-Mev π^-	465-Mev π^-	1.5-Bev π^-	210-Mev π^+
π	0.365±0.022	0.351±0.020	0.828±0.037	1.992±0.072	0.361±0.021
π^0	0.100±0.012	0.127±0.012	0.249±0.020	0.881±0.048	0.120±0.012
π^+	0.003±0.002	0.001±0.001	0.055±0.009	0.196±0.023	0.033±0.006
π^-	0.263±0.019	0.223±0.015	0.524±0.029	0.915±0.049	0.207±0.016
n	1.156±0.040	1.309±0.037	1.829±0.055	4.34 ±0.11	1.174±0.037
p	0.369±0.023	0.492±0.023	1.006±0.041	2.532±0.081	1.206±0.038
$n+p$	1.525±0.046	1.801±0.044	2.836±0.068	6.86 ±0.13	2.380±0.053
p/n	0.32 ±0.02	0.38 ±0.02	0.55 ±0.03	0.58 ±0.03	1.03 ±0.05

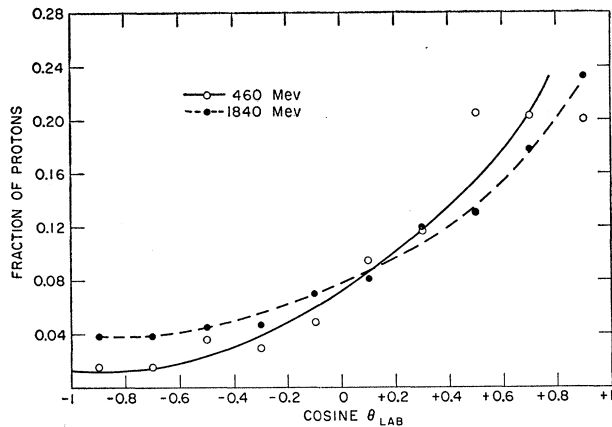


FIG. 6. Angular distribution of protons with kinetic energies between 30 and 90 Mev emitted in the bombardment of aluminum with protons of 460 Mev (294 protons included) and 1840 Mev (491 protons included). The ordinate scale gives fraction of protons per 0.2 interval in $\cos\theta$.

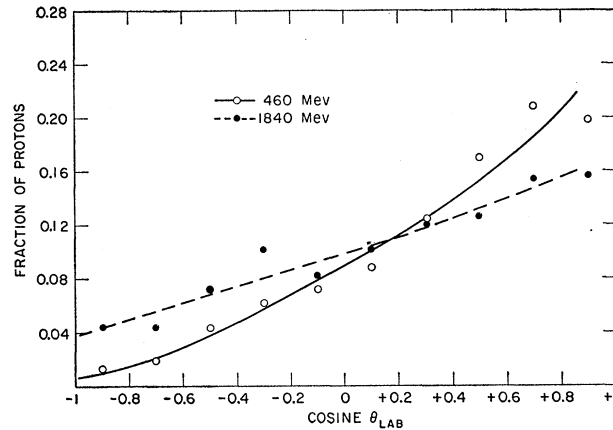


FIG. 8. Angular distribution of protons with kinetic energies between 30 and 90 Mev emitted in the bombardment of uranium with protons of 460 Mev (300 protons included) and 1840 Mev (522 protons included). The ordinate scale gives fraction of protons per 0.2 interval in $\cos\theta$.

target nuclei. Data from I are included. Three outstanding features are apparent from this figure:

- (i) The average excitation energy at any given bombarding energy increases with the mass number of the target nucleus.
- (ii) The average excitation energy increases only slowly with the incident particle energy for energies below about 350 Mev.
- (iii) The average excitation energy increases relatively rapidly with incident energy for incident energies above about 400 Mev.

The first feature is a clear consequence of the decreasing probability for the escape of cascade nucleons as the size of the nucleus increases. It is quite consistent with the result, illustrated in Fig. 4, that the number of

emitted cascade nucleons is rather insensitive to mass number and, indeed, decreases slightly with increasing mass number for incident energies below about 1 Bev.

The second feature is a consequence of the fact that the nucleon-nucleon interaction cross sections decrease with increasing energy in this energy region; therefore, the escape probability for cascade nucleons increases.

The rather pronounced increase in the rate of change of residual excitation energy with bombarding energy that occurs around 400-Mev incident energy is the result of the emergence of a new and efficient mechanism for the transfer of kinetic energy of fast nucleons to excitation energy of the residual nucleus, namely meson production and subsequent meson interactions. This process is a more efficient energy transfer mechanism than the purely elastic nucleonic

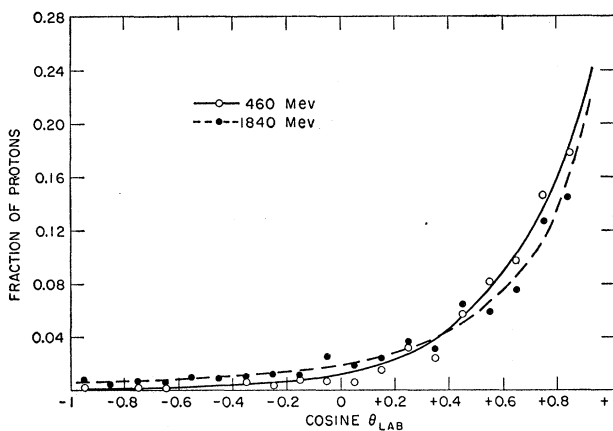


FIG. 7. Angular distribution of protons with kinetic energies greater than 90 Mev emitted in the bombardment of aluminum with protons of 460 Mev (512 protons included) and 1840 Mev (880 protons included). The ordinate scale gives fraction of protons per 0.1 interval in $\cos\theta$.

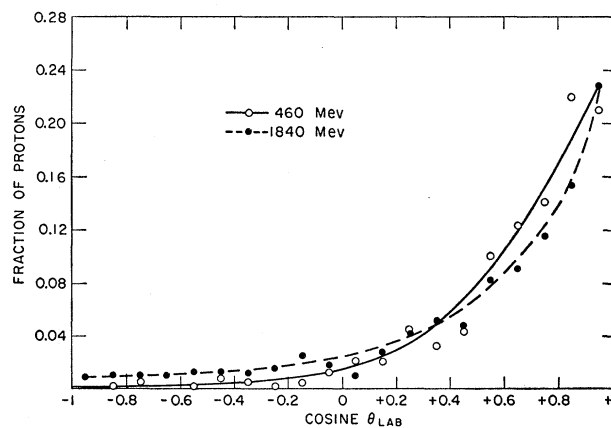


FIG. 9. Angular distribution of protons with kinetic energies greater than 90 Mev emitted in the bombardment of uranium with protons of 460 Mev (388 protons included) and 1840 Mev (610 protons included). The ordinate scale gives fraction of protons per 0.1 interval in $\cos\theta$.

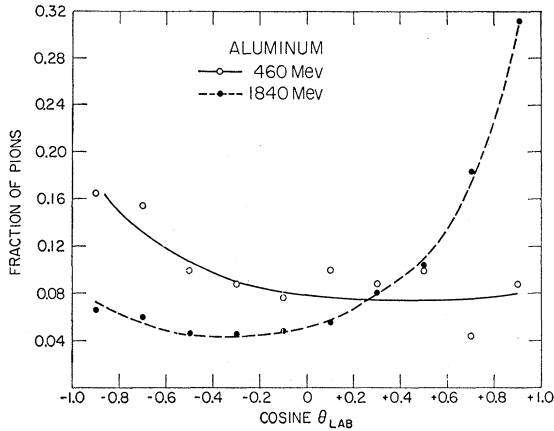


FIG. 10. Angular distribution of pions (all charge states and all energies) emitted in interactions of aluminum with protons of 460 Mev (91 pions emitted) and 1840 Mev (592 pions emitted). Ordinate scale gives fraction of pions per 0.2 interval in $\cos\theta$.

cascade because in nuclear matter the scattering mean free path of a pion created in a nucleon-nucleon collision is generally shorter than that of the nucleon that produced the pion. Further, the pion has an appreciable probability of being reabsorbed, thereby effectively transferring a large part of the kinetic energy of a single high-energy cascade nucleon to at least three others: the partner in the production process and the two nucleons participating in the absorption of the pion. Actually, more than three nucleons will share in the transferred energy because of the high probability for several scatterings of the pion before it is absorbed. The curves shown in Fig. 14 suggest that the onset of double pion production may contribute to the further increases in average excitation with increasing bombarding energy above 1 Bev.

The mass spectrum of residual nuclei and their average excitation energies.—In Fig. 15 we show the dependence upon incident energy of the cross section for forming excited residual nuclei of various mass numbers in the proton irradiation of copper-64. The data obtained with other targets are in general quite similar to these.

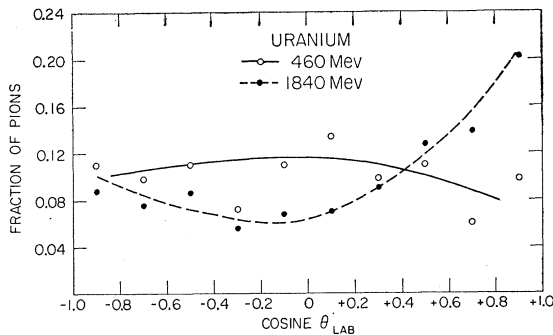


FIG. 11. Angular distribution of pions (all charge states and all energies) emitted in interactions of uranium with protons of 460 Mev (82 pions emitted) and 1840 Mev (442 pions emitted). Ordinate scale gives fraction of pions per 0.2 interval in $\cos\theta$.

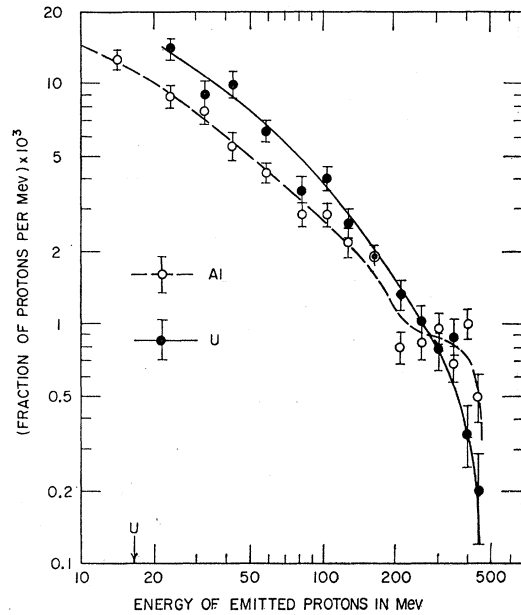


FIG. 12. Energy spectra of cascade protons emitted when 460-Mev protons are incident on aluminum and uranium nuclei. The arrow marked U indicates the lowest kinetic energy with which protons can emerge from a uranium nucleus according to the assumptions of the calculation. The corresponding cutoff energy for Al is at 4.6 Mev.

Figure 16 exhibits the dependence of the average excitation of various residual nuclei upon the bombarding energy in the irradiation of copper-64. It may be noted that, at a given incident energy, the mean

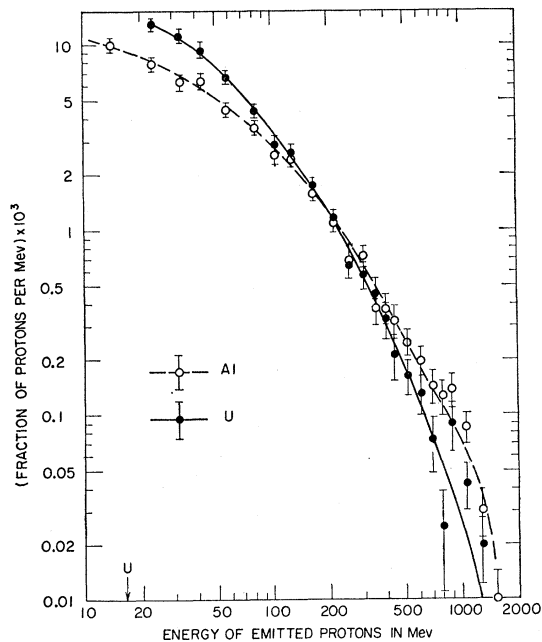


FIG. 13. Energy spectra of cascade protons emitted when 1840-Mev protons are incident on aluminum and uranium nuclei. As in Fig. 12, the arrow marks the cutoff energy for protons from U.

TABLE XI. Fraction of pions emitted in each of four energy intervals when copper and uranium nuclei interact with protons of several energies.

Pion energy (Mev)	Copper			Uranium		
	460 Mev	940 Mev	1840 Mev	460 Mev	940 Mev	1840 Mev
0-45	0.48	0.27	0.23	0.47	0.37	0.26
45-90	0.44	0.25	0.19	0.42	0.25	0.19
90-200	0.06	0.13	0.09	0.11	0.09	0.11
>200	0.02	0.35	0.49	0.00	0.29	0.44

excitation of residual nuclei increases almost linearly with the number of cascade nucleons emitted. This result is in some respects surprising but it is not unreasonable on the grounds that proliferation of the cascade results both in the emission and in the retention of a larger number of cascade nucleons. Another striking feature is the small slope of the curves of Fig. 16 once the incident energy exceeds what may be called the threshold for forming a given residual nucleus in the cascade. As might be expected, the excitation energy deposited in a cascade characterized by a given number of emitted nucleons (i.e., by a given ΔA) increases with nuclear size. This is illustrated in Fig. 17 where the average excitation corresponding to a few ΔA values is plotted against target mass number for two incident proton energies.

The excitation energy spectrum of residual nuclei.—The excitation-energy spectra of several different residual nuclei produced by protons incident upon copper-64 are shown in Fig. 18. As might be expected, the spread in the excitation-energy spectrum as well as the average excitation increases with increasing number of emitted cascade particles. The spectrum for a given cascade product does not appear to depend strongly on incident energy.

COMPARISONS WITH EXPERIMENT

Unfortunately there are at present not many experimental data with which the results of the cascade

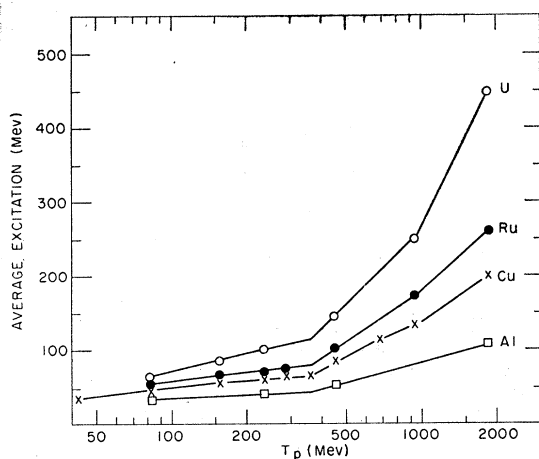


FIG. 14. Average excitation energy in residual nucleus, plotted as a function of incident proton energy for four target elements.

calculations can be compared. The following comparisons, however, serve to demonstrate the general usefulness of the model in the energy range under discussion, to point up some specific discrepancies between the predictions of the present calculations and experimental observation, and perhaps to indicate how some of these shortcomings of the calculation might be removed by refinements in assumptions and parameters.

Interaction of 950-Mev protons with silver and bromine.—Lock, March, and McKeague⁴³ have studied the nuclear disintegrations of heavy emulsion nuclei by 950-Mev protons, and their data can be compared in some detail with the results of the present calculation for 940-Mev protons incident on Ru¹⁰⁰. Some difficulty arises from the experimental problem of eliminating interactions in light nuclei (C, N, O), which Lock *et al.* do⁴⁴ by assigning to such disintegrations those and only those stars which have nine prongs or less and which contain at least one track between 10 and 50 μ in length. This second criterion is based on the idea that particles of such short range can, in general, not penetrate the Coulomb barriers of heavy emulsion nuclei. However, as the authors themselves recognize,⁴⁴ some events in light nuclei will also not be accompanied by the emission of particles of range less than 50 μ and will thus be

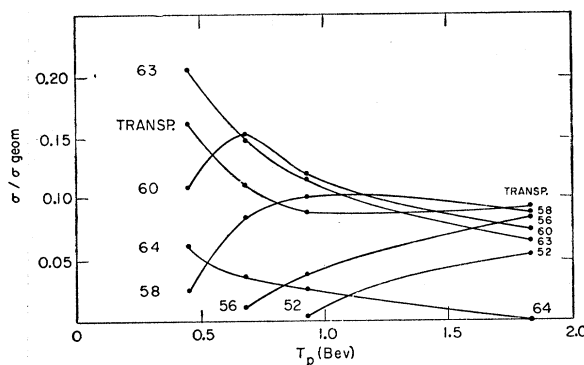


FIG. 15. Cross sections (relative to the geometric cross section) for the formation of cascade residues of various mass numbers in the interactions of Cu⁶⁴ nuclei with protons of different energies. The curve marked "Transp." shows the transparencies, that marked "64" represents those cascades in which a nucleus of mass number 64 results, but with residual excitation; the other numbers indicate other residual A values.

⁴³ Lock, March, and McKeague, Proc. Roy. Soc. (London) A231, 368 (1955).

⁴⁴ Lock, March, Muirhead, and Rosser, Proc. Roy. Soc. (London) A230, 215 (1955).

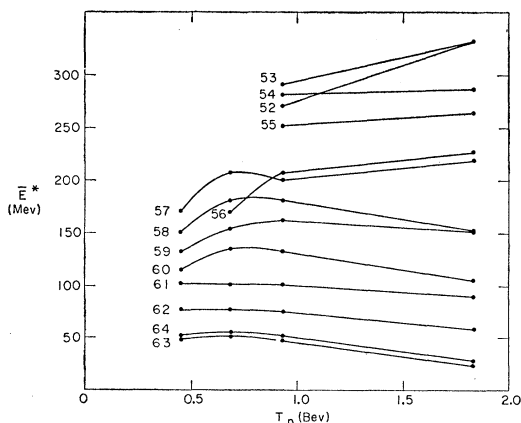


FIG. 16. Average excitation energy of various residual nuclei formed in the interaction of Cu^{64} with protons, as a function of incident energy. The numbers indicate the mass numbers of the residual nuclei.

misassigned as heavy-element interactions. This effect will be the more important, the smaller the prong number. The facts that Lock *et al.*⁴³ assign only 2 out of 292 events with ≤ 2 prongs and only 8% of all stars (instead of the 20 or 25% expected from the emulsion

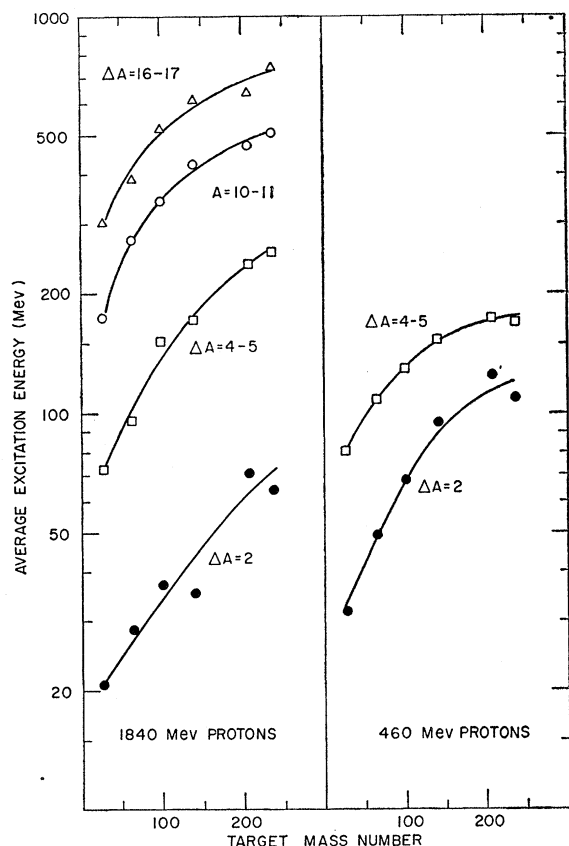


FIG. 17. Average excitation energies corresponding to various mass changes plotted as a function of target mass for two incident proton energies.

TABLE XII. Comparison of calculated and observed mean numbers of particles ejected per star from heavy nuclei disintegrations in emulsions. (Experimental data from reference 43.)

	Experimental	Present calculation
Shower particles	0.54 ± 0.04	0.30 ± 0.02
Gray prongs	1.11 ± 0.07	1.77 ± 0.05
Black prongs	2.61 ± 0.11	3.55 ± 0.07
Total	4.26 ± 0.18	5.62 ± 0.09
Charged pions	0.18 ± 0.05	0.30 ± 0.02

composition) to light-element interactions almost certainly result from such incorrect identifications.

If the above analysis is correct it may account for the deficiency of one- and two-pronged events predicted by the MANIAC calculation as compared to Lock's data. The comparison of calculated and measured prong distributions is shown in Fig. 19 in two ways. In graph (A) the histograms are normalized to the total number of events, in graph (B) to the number of events with 3 or more prongs, for which the scanning criteria should be more nearly correct. It is seen that the agreement is very good for prong numbers of 3 or greater. The calculated prong distribution includes a contribution (about 50% of all particles) from evaporation prongs, computed on the basis of each 50 Mev of excitation energy giving rise to a charged evaporation particle.⁴⁵ The discrepancy in frequency of one- and two-pronged events almost completely accounts for the difference between the over-all mean prong number per star as given by Lock⁴³ (4.26 ± 0.18) and that deduced from

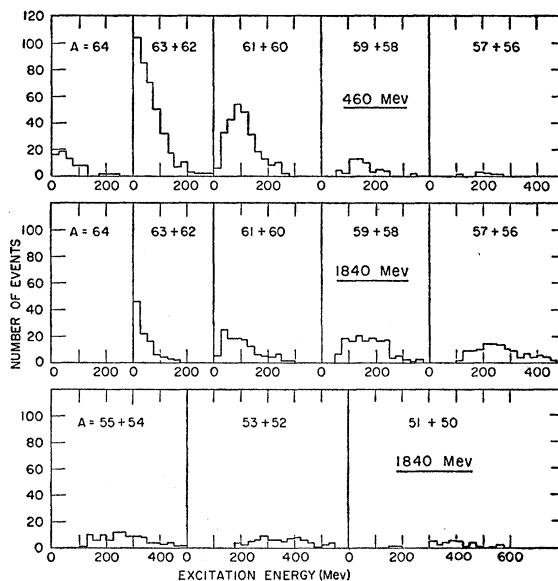
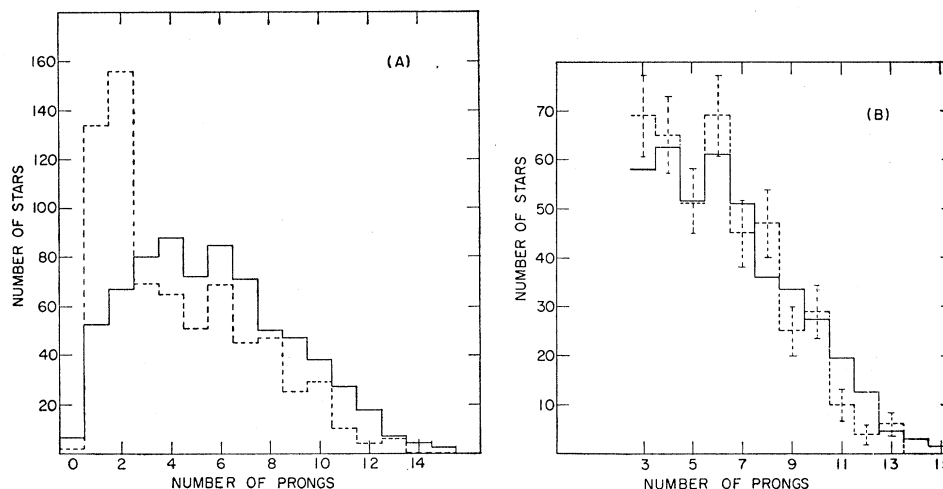


FIG. 18. Excitation energy spectra for different cascade products from the bombardment of Cu^{64} with protons of 460-Mev and 1840-Mev incident energy. Cascade products of neighboring mass numbers are grouped together.

⁴⁵ K. J. LeCouteur, Proc. Phys. Soc. (London) A63, 259 and 498 (1950), A65, 718 (1952); and Dostrovsky, Bivins, and Friedlander (unpublished calculations).

FIG. 19. Comparison of calculated and measured prong distributions resulting from the interaction of 950-Mev protons with heavy emulsion nuclei. The solid histograms represent the results of the MANIAC calculation for 940-Mev protons incident on Ru¹⁰⁰, the dashed histograms are the data of Lock *et al.* from reference 43. In graph (A) the two sets of data are normalized to the total number of events, in graph (B) to the number of events with 3 or more prongs.



the present calculations (5.62 ± 0.09). It is not so clear what causes the disagreement found when one compares the measured and calculated mean prong numbers in three separate energy intervals as is done in Table XII. Here, following Lock's analysis and terminology, shower particles mean protons of kinetic energy greater than 450 Mev and charged pions above 68 Mev, gray prongs designate protons between 30 and 450 Mev and pions between 4.5 and 68 Mev, and black prongs are those protons and pions of still lower energy. For the purpose of constructing Table XII, all evaporation particles were assumed to be black prongs. The errors given are standard deviations corresponding to the statistical reliability of the numbers of events found.

The mean number of charged pions emitted per interaction (see Table XII) appears to be somewhat overestimated by the MANIAC calculation. This may well be due to the assumptions made about energy

distribution in elementary pion production processes; these assumptions tend to result in an overestimate of high-energy pions which have relatively large mean free paths in nuclear matter. It may also be significant that Lock *et al.*⁴⁴ found no pions emitted from stars with 10 or more prongs, whereas the analysis of the MANIAC data shows $(12 \pm 3)\%$ of all the charged pions to originate from such large stars.

The angular distributions of shower particles and gray tracks reported by Lock *et al.* are compared with the results of the Monte Carlo calculations in Fig. 20. Each set of histograms has been normalized to the same total area. The agreement is excellent except for the deficiency of very small angles ($0-10^\circ$) in the calculated

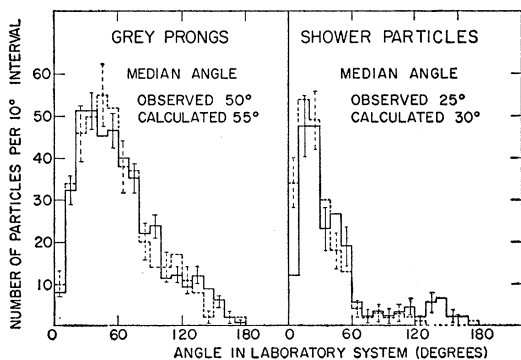


FIG. 20. Angular distributions of gray prongs and shower particles resulting from the interaction of 950-Mev protons with heavy emulsion nuclei. The dashed histograms are the data of Lock *et al.* from reference 43, the solid histograms represent the results of the MANIAC calculation normalized to the observed number of prongs. The abscissa is the space angle between the outgoing particle and the incident beam direction. Standard deviations are given for the calculated and measured values in alternate angular intervals.

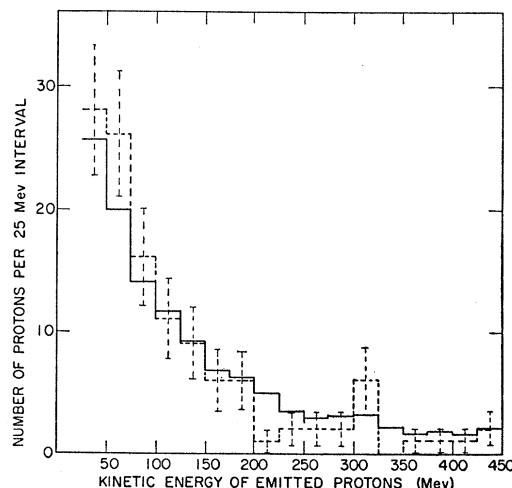


FIG. 21. Energy spectrum of gray prongs resulting from the interaction of 950-Mev protons with heavy emulsion nuclei. The dashed histogram represents the data of Lock *et al.* (reference 43), the solid histogram gives the results of the present calculation, normalized to the experimentally observed number of particles and including about 7% pions plotted at equivalent proton energies. The standard deviations for the experimental data only are given; those of the calculated numbers are somewhat smaller.

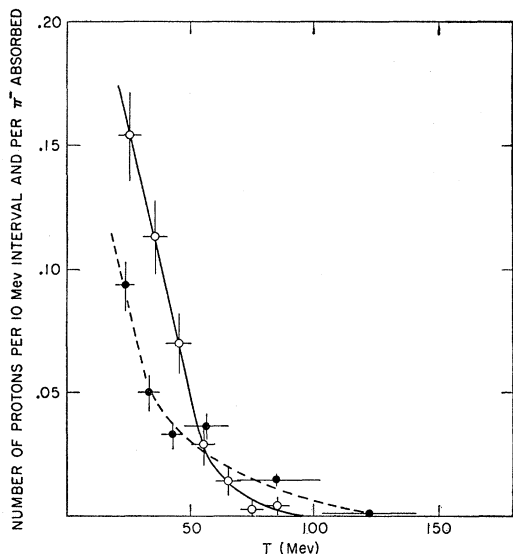


FIG. 22. Kinetic energy distribution of fast protons produced when slow π^- mesons are absorbed in heavy nuclei. The results of the present calculation for Ru^{100} (full circles) are compared with the experimental data of reference 46 on Ag and Br interactions (open circles).

distribution of shower particles. The angular distributions are, of course, much less sensitive to the possible misassignment of light-element events to Ag and Br than are the prong distributions. It should also be mentioned that, according to the calculations, the contribution of pions to the gray prongs is only 7%, whereas pions constitute 60% of the shower particles.

Figure 21 shows a comparison of the calculated and observed energy spectra of gray prongs. For this purpose the pion kinetic energies from the Monte Carlo data were converted to equivalent proton kinetic energies (by multiplication by the ratio of rest masses). This corresponds to the experimental procedure in which the energies were deduced from grain density under the

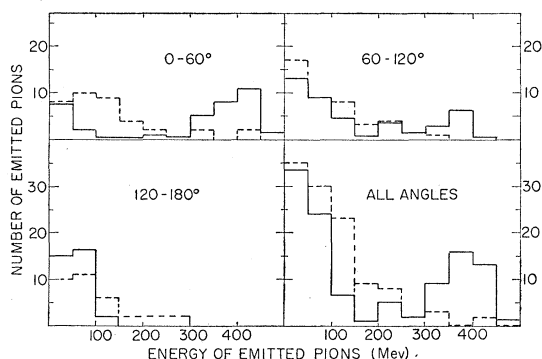


FIG. 23. Comparison between calculated and measured energy spectra of charged pions emitted in the interaction of negative pions with nuclei. The solid histograms represent the MANIAC data for 465-MeV π^- mesons incident on Ru^{100} , the dashed lines are the data of Blau and Caulton for 500-MeV π^- interactions with Ag and Br in emulsions. Spectra in three angular intervals as well as the over-all spectrum are shown.

assumption that all gray tracks were proton tracks. The agreement between calculation and experiment is very satisfactory.

Absorption of slow π^- mesons in silver and bromine.—To provide a test of the pion absorption mechanism assumed, cascade calculations were performed to simulate slow π^- absorption by complex nuclei. Here each cascade was started by having a π^- meson with zero kinetic energy absorbed at a random location within the nucleus. The fast nucleons produced in the absorption process were followed in the usual manner and the numbers and energy spectra of emitted cascade protons were compared with experimental nuclear emulsion data. The most recent study of this type is that on σ stars produced by π^- mesons reported by Azimov *et al.*⁴⁶ These authors indicate that earlier work⁴⁷ may have been in error in underestimating the number of fast (>30 Mev) protons. The average number of such fast protons emitted per π^- absorbed is calculated to be 0.187 ± 0.013 ; the experimental result of Azimov *et al.* (assuming that 28% of all incident π^- mesons result in interactions without charged particle emission^{47,48}) is 0.143 ± 0.013 . The average kinetic energy of these fast protons is calculated to be 57 Mev; that observed is 43 Mev. The calculated and observed energy distributions for protons having energy greater than 20 Mev are presented in Fig. 22.

These comparisons indicate only qualitative agreement of the present Monte Carlo calculations with experiment. The deviations are significant and indicate deficiencies in the model of π^- absorption used—at least at these low energies. Three possible reasons for the lack of agreement between the calculations and experiments are:

- (1) Absorption of such low-energy π^- mesons may occur at least part of the time on more complex aggregates inside the nucleus—such as α particles.
- (2) There may be some preference for absorption on (PN) pairs as contrasted with (PP) pairs. This has been postulated earlier by DeSabbata, Manaresi, and Puppi⁴⁹ and by Tomasini⁵⁰ who performed simplified Monte Carlo calculations to compare with their emulsion data on slow π^- absorption and found discrepancies similar to those discussed here.
- (3) Absorption may occur preferentially on low-energy nucleons inside the nucleus.

Interaction of 500-MeV π^- mesons with silver and bromine nuclei.—The experimental results from Blau

⁴⁶ Azimov, Gulianov, Zanichalova, Nizametdinova, Podgoret-skii, and Imidashev, J. Exptl. Theoret. Phys. U.S.S.R. **31**, 756 (1956) [translation: Soviet Phys. JETP **4**, 632 (1957)].

⁴⁷ Menon, Muirhead, and Rochat, Phil. Mag. **41**, 583 (1950).

⁴⁸ Gardner, Barkas, Smith, and Bradner, Science **111**, 191 (1950).

⁴⁹ DeSabbata, Manaresi, and Puppi, Nuovo cimento **10**, 1704 (1953).

⁵⁰ A. Tomasini, Nuovo cimento **3**, 160 (1956).

TABLE XIII. Comparison of MANIAC results on 465-Mev π^- interactions with Ru^{100} with the experimental data of Blau and Caulton^a obtained with 500-Mev π^- mesons incident on AgBr.

		Experimental	Present calculations
1. Fraction of events with n charged pions emitted	$\left\{ \begin{array}{l} n=0 \\ 1 \\ 2 \end{array} \right.$	0.60 0.38±0.06 0.01±0.03	0.53 ±0.04 0.43 ±0.03 0.032±0.009
2. Average number of "black prongs" per star. (Assume 50-Mev excitation per evaporation prong)	$\left\{ \begin{array}{l} \text{Stars with } \pi^\pm \\ \text{Stars without } \pi^\pm \end{array} \right.$	2.7 ±0.1 4.3 ±0.2	2.7 ±0.2 4.1 ±0.3
3. Fraction of stars with at least one fast (>30 Mev) proton	$\left\{ \begin{array}{l} \text{Stars with } \pi^\pm \\ \text{Stars without } \pi^\pm \end{array} \right.$	0.40 0.66	0.40 ±0.05 0.66 ±0.06
4. Mean energy of emitted π^\pm		110 Mev	174 Mev

^a Reference 51.

and Caulton's investigation⁵¹ of the interaction of 500-Mev negative pions with the silver bromide in nuclear emulsion are compared in Table XIII and Figs. 23 and 24 with the results of the present calculations for 465-Mev negative pions incident upon ruthenium-100. In the analysis of the Monte Carlo data each cascade was assigned a statistical weight equal to the scanning efficiency given by Blau and Caulton to the corresponding type of event in the emulsion. This correction has a significant effect upon the degree of agreement found.

The comparison between experiment and calculation given in Table XIII shows excellent agreement for the frequencies of various types of events, but the calculated average kinetic energy (174 Mev) of the outgoing charged pions is significantly larger than that observed (110 Mev). In Fig. 23 the energy spectra of emitted charged pions are shown, both for all angles and separately for three angular intervals. Here it can be seen that the discrepancy in average energy noted above arises primarily from the relatively large number of events with small energy loss and small scattering angles predicted by the calculation. The introduction of a pion-nuclear potential (especially a velocity-dependent one) would certainly alter the calculated spectrum of emitted pions, presumably in the desired direction (see the following section). However, without additional calculations it is not clear whether agreement with the experimental data could be obtained in this way. It should perhaps be pointed out that the discrepancy could also, at least in part, arise from experimental difficulties. Small-angle scatterings with small energy losses might have been missed in the scanning.

A comparison of calculated and observed angular distributions of emitted pions as illustrated in Fig. 24 again shows the same difficulty, namely an excess of small-angle scatterings in the calculation as compared with Blau and Caulton's data. There also appears to be a deficiency in the calculated number of pions emitted at angles greater than 150° to the beam direction.

Interaction of 162-Mev negative pions with silver and bromine nuclei.—Nikol'skii *et al.*² have investigated the

⁵¹ M. Blau and M. Caulton, Phys. Rev. **96**, 150 (1954).

inelastic interactions of 162-Mev negative pions with the silver and bromine nuclei in photographic emulsions. Through a comparison of their experimental results with a simplified Monte Carlo calculation, they concluded that an attractive nuclear potential for pions should be included in a model constructed to represent these interactions. A comparison of their experimental results with the MANIAC calculation has been made by very small interpolations and extrapolations of the MANIAC results for 134-Mev and 179-Mev negative pions incident on Ru^{100} .

The observed energy spectrum of charged pions emitted in the backward direction is compared with that obtained from the present calculation in Fig. 25(A). There it is again seen that the calculation gives too many high-energy pions; but the discrepancy between calculation and experiment is not as large as it is for incident negative pions of 500-Mev kinetic energy. The effect upon the calculated spectrum of an attractive pion-nucleus potential of V Mev was investigated as follows: V Mev was subtracted from the

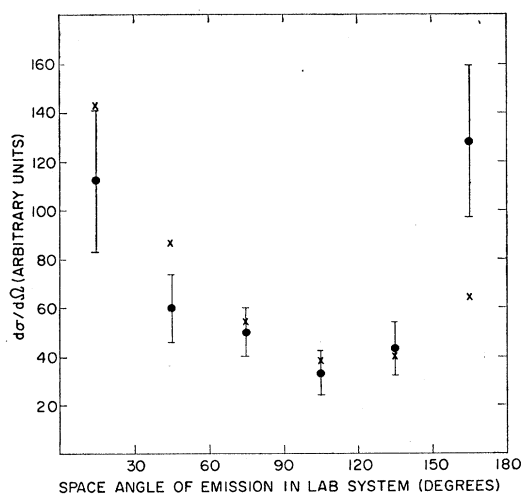


Fig. 24. Comparison between calculated and measured angular distributions of charged pions emitted in the interaction of negative pions with nuclei. The MANIAC data for 465-Mev π^- interactions with Ru^{100} (crosses) are compared with the results of Blau and Caulton on 500-Mev π^- mesons incident on Ag and Br (solid circles).

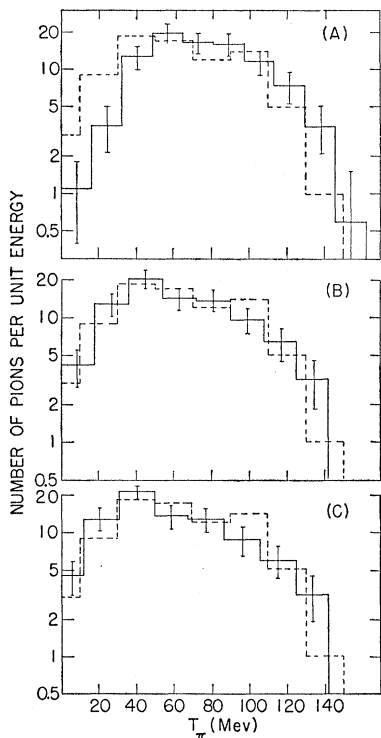


FIG. 25. Energy spectrum of charged pions emitted in the interaction of 162-Mev π^- mesons with heavy emulsion nuclei. The experimental data of Nikol'skii *et al.* (dashed) are compared with the results of the present calculation for Ru^{100} (solid). The calculations were made with three different assumptions about pion-nucleus potential: no potential (A), 18-Mev attractive potential (B), and 26-Mev attractive potential (C).

kinetic energy of each pion emitted in an interaction induced by a pion with energy of $(162+V)$ Mev; those pions that would thus be emitted with negative kinetic energies were assumed to be absorbed. In this manner the spectra corresponding to attractive potentials of 18 Mev and 26 Mev were constructed; they are compared with Nikol'skii's experimental data in Figs. 25(B) and (C). It is seen that the observed energy distribution is reproduced fairly well when an attractive potential for pions is included in the model. A potential of 18 Mev gives perhaps a slightly better fit than one of 26 Mev; in any case the present result is in agreement with the conclusion of Nikol'skii *et al.*² that the data can be fitted with an attractive potential of 24 ± 6 Mev.

The counter data of Miller⁵² on the inelastic scattering of 150-Mev π^- mesons from C and Pb are, as the author points out, also inconsistent with the predictions of the model used here without a pion-nucleus potential. The predicted average energy of the pions scattered in the backward direction is much higher than observed. The introduction of an attractive potential here would again probably decrease the disagreement, but MANIAC data on pion-induced C and Pb cascades are at present not available for comparison.

⁵² R. H. Miller, *Nuovo cimento* **6**, 882 (1957).

Although the introduction of a pion-nucleus potential appears adequate to explain the energy distribution of inelastically scattered pions found by Nikol'skii *et al.*² the over-all angular distribution of the pions does not appear to be well represented by the present model, with or without a potential. The calculations predict a much stronger angular asymmetry (backward peaked) than is observed. Introduction of an attractive pion-nucleus potential into the model reduces the disagreement; but even the MANIAC results corresponding to a 17-Mev potential are quite a poor representation of the experimental data, as shown in Fig. 26. It appears that a much larger potential would be required to obtain agreement, probably too large to be compatible with the energy spectrum data. Whether the agreement would be improved by use of a nuclear model with a diffuse boundary as Nikol'skii *et al.*² suggest, has not been tested yet.

Spallation of copper with 2-Bev protons.—The results of radiochemical studies of spallation cross sections can in general be compared with the cascade calculations only if estimates of the cross sections for unobserved spallation products are made (some products are not observed because they are stable or have either very short or very long half-lives), and if the number of particles "evaporated" from the various excited nuclei remaining after the prompt cascade is also estimated. The mass-yield curve for the spallation of copper with 2.2-Bev protons found experimentally by Friedlander *et al.*⁵³ is compared in Fig. 27 with that predicted by the

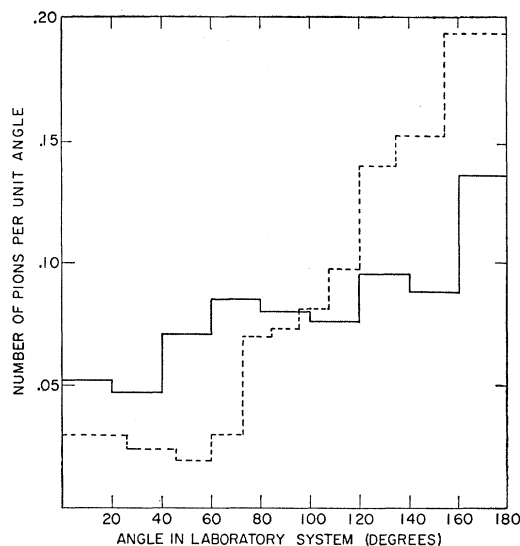


FIG. 26. Angular distribution of charged pions emitted in the interaction of 162-Mev π^- mesons with heavy emulsion nuclei. The experimental data of Nikol'skii *et al.* (solid) are compared with the results of the present calculation incorporating an attractive pion-nucleus potential of 17 Mev (dashed). The two sets of data are normalized to the same total number of emitted pions. The ordinate scale is arbitrary.

⁵³ Friedlander, Miller, Wolfgang, Hudis, and Baker, *Phys. Rev.* **94**, 727 (1954).

MANIAC calculation for 1.84-Bev protons. The experimental curve includes estimates of unobserved cross sections made on the basis of rather crude evaporation theory calculations giving relative isobaric yields.⁵⁴ The number of particles emitted by the excited nuclei remaining after the cascade was crudely estimated as follows: no evaporation was assumed for excitations below 10 Mev, loss of one mass number for excitations between 10 and 25 Mev, and loss of one additional mass number for every 0 to 17 Mev beyond 25 Mev. The adjustments that have been applied to both the experimental and calculated results are quite approximate, and details such as the magnitude and position of the slight maximum in the adjusted experimental mass-yield curve should not be taken too seriously. Nevertheless, the general form of both curves could not be altered seriously by a more refined treatment, and the rather good agreement between the calculation and the experimental results in Fig. 27 would probably persist. In this connection, attention should be called to the fact that the very differently shaped mass-yield curve for copper spallation with 340-Mev protons is also well reproduced by the Monte Carlo calculations (Fig. 22 of I). At both energies the present calculation underestimates the cross section for a mass change of one unit [(p,pn) and $(p,2p)$ reactions] by a factor of about 3. This discrepancy appears to exist for (p,pn) reactions in general and, as already mentioned in I, may at least in part result from the assumption of a sharp nuclear boundary.

The comparisons presented indicate that the extension of the nuclear cascade calculations into the energy region where pion processes are important is reasonably successful. Many features of the experimental observations are reproduced at least semi-

⁵⁴ The production cross section of 27 mb for V^{49} quoted in reference 53 was based on a half-life of 600 days. For the mass yield curve of Fig. 27, a 15-mb cross section for V^{49} was used, on the basis of recent half-life measurements of 330 days.

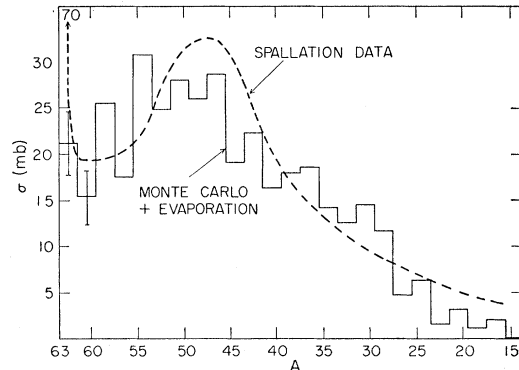


FIG. 27. Mass-yield curve for the products formed in the interaction of copper with protons of about 2 Bev. The results of the present calculations for 1.84-Bev protons on Cu^{64} supplemented by a crude evaporation calculation (solid histogram) are compared with the data of reference 53 on 2.2-Bev proton interactions with copper (dashed curve).

quantitatively. Others are not, and the nature of these disagreements may indicate certain refinements in the model used which should be tried. Among these are a pion-nucleus potential, a diffuse nuclear boundary, a better approximation to the kinematics of π -production events, and changes in the assumptions about the pion absorption mechanism.

ACKNOWLEDGMENTS

The authors are indebted to a large number of colleagues for helpful discussions. The cooperation of J. Richardson and W. Orvedahl of the MANIAC engineering staff was indispensable. Dr. R. H. Miller kindly made his data on pion interactions available before publication. Dr. Brian Pate's detailed criticism of the manuscript is gratefully acknowledged. Dr. J. Hudis, Mrs. E. McIver, Mrs. P. Payne, and Miss K. Brennan were most helpful in the compilation and statistical analysis of the MANIAC results.